PHYSICAL REVIEW B

CONDENSED MATTER

THIRD SERIES, VOLUME 47, NUMBER 6 1 FEBRUARY 1993-II

Constant-volume pair potential for Al–transition-metal compounds

J. Zou and A. E. Carlsson

Department of Physics, Washington University, One Brookings Drive, St. Louis, Missouri 63130

(Received 22 June 1992; revised manuscript received 8 October 1992)

We treat the problem of two transition-metal atoms embedded in Al by means of a simple *s-d* model Hamiltonian with localized *d* orbitals. A Green's-function analysis gives the electronic density of states and total energy as functions of the separation between the two transition-metal atoms. The pair potential thus obtained is strong and has Ruderman-Kittel-Kasuga-Yosida-type oscillations as its asymptotic behavior. It is applicable to cases in which transition metals are not nearest neighbors. With this pair potential, we calculate the structural energy differences of Al_3M compounds in the $L1_2$ and DO_{22} structures, where M includes all of the group III, IV, V transition metals and the whole 4*d* row. Comparison with *ab initio* results reveals good agreement for the transition metals in group V and beyond, but not for the earlier transition metals, in which the *p-d* covalent bonding and three-body interactions are likely more important. We also calculate the (100) antiphase boundary (APB) energies for Al_3V, Al_3Nb, and Al_3La, and find a strong correlation between the APB energy and the structural energy difference. The low-order moment-expansion method is used to obtain short-ranged potentials in an effort to obtain better convergence for the structural energies. This approach fails, giving magnitudes for the structural energy differences that are much too small.

INTRODUCTION

The wide range of potential uses of transition-metal aluminides in applications requiring high strength and light weight has stimulated a large number of atomistic simulations of extended defects in these systems.[1–4] It is hoped that such simulations can elucidate the causes of the brittleness of the aluminides, and, hopefully, suggest ways of circumventing this brittleness. Except for highly symmetric defects, all of the simulations have been performed using simplified potential-energy functions, with particular emphasis on the embedded-atom method (EAM).[5–12] The EAM gives a good accounting for the environmental dependence of the effective bond strengths in metals, but does not accurately treat long-ranged electronic effects. *Ab initio* calculations[13,14] have shown that these effects are important in determining the structural energies of aluminides; the structural energies are in turn closely related to antiphase boundary (APB) energies, which have a strong impact on dislocation and grain-boundary structure. The long-ranged electronic effects have been included in Ising-type interactions obtained via the "Generalized Perturbation Theory".[15–17] These, unfortunately, are only applicable when all of the atoms reside on an underlying Bravais lattice that is fixed. Therefore they cannot be used directly in simulations of extended defect properties, although the method could be extended to defect configurations. The aim of our work is to establish the strengths and limitations of a simple pair-potential description which does not require underlying structural periodicity. In this way, we hope to establish the functional form of terms which might be added to EAM-type formulations in order to improve the treatment of structural energies and APB properties. Our basic approach is the use of a constant-volume constraint, which in simple metals allows the calculation of a pair potential via a perturbation expansion in the strength of the pseudopotential.[18] This approach has subsequently been extended to transition metals by Harrison and Moriarty.[19–23] Our method is essentially a simplified, parametrized form of Moriarty's method, using input from *ab initio* band calculations to fix the parameters. This allows us to isolate the effects of the *d-d* interactions, and to obtain a simple parametrized form for the pair potential.

METHOD

We consider the following problem: two transition-metal atoms *a* and *b*, a separation **R** apart from each other in an Al-like environment. We use a simple Hamiltonian in which the *s-p* electrons are free, and the transition-metal *d* orbitals are noninteracting and orthogonal to the *s-p* plane waves:

$$H=\sum_{\mathbf{k}}\varepsilon_{\mathbf{k}}|\mathbf{k}\rangle\langle\mathbf{k}|+\sum_{m=-2}^{2}\varepsilon_d|a,m\rangle\langle a,m|+\sum_{m=-2}^{2}\varepsilon_d|b,m\rangle\langle b,m|$$
$$+\sum_{\mathbf{k},m}[V_{\mathbf{k}am}|\mathbf{k}\rangle\langle a,m|+\text{H.c.}]+\sum_{\mathbf{k},m}[V_{\mathbf{k}bm}|\mathbf{k}\rangle\langle b,m|+\text{H.c.}]\ , \tag{1}$$

with

$$V_{\mathbf{k}bm}=\exp(-i\mathbf{k}\cdot\mathbf{R})V_{\mathbf{k}am}\ . \tag{2}$$

This is essentially a two-impurity Anderson model with orbital degeneracy included. Here $\varepsilon_{\mathbf{k}}$ is the energy of the free-electron state $|\mathbf{k}\rangle$; ε_d is the energy of the transition-metal atomic d states; $V_{\mathbf{k}am}$ and $V_{\mathbf{k}bm}$ are the hybridization matrix elements between $|\mathbf{k}\rangle$ and d states. Our assumptions require that $\langle a,m|b,m'\rangle=0$ for all m,m', and that $\langle a,m|\mathbf{k}\rangle=0$, $\langle b,m|\mathbf{k}\rangle=0$ for all m and $\mathbf{k}$. For convenience, we refer to $|a,m\rangle$, $|b,m\rangle$ as $|d\rangle$, and the set of $|d\rangle$ plus $|\mathbf{k}\rangle$ as $|\alpha\rangle$. Moriarty has treated the d-band metals with pseudo-Green's functions and pseudopotential theory.[21] Our model Hamiltonian in this paper is similar to his. The major difference is that Moriarty treated $|\alpha\rangle$ as an overcomplete set, because the plane waves $|\mathbf{k}\rangle$ themselves form a complete set, so that there must be some overlap between $|\mathbf{k}\rangle$ and $|d\rangle$. In fact, the nonorthogonality can be treated within the orthogonal formalism by introducing effective energy-dependent hybridizations. Suppose the nonorthogonal basis set $|\alpha\rangle$ has overlap matrix S and coupling matrix V. One sees readily that we can treat $|\alpha\rangle$ as an orthonormal set if we replace V by a generalized energy-dependent matrix:

$$V'(E)=V-ES\ , \tag{3}$$

or

$$V'(E)=V'(\varepsilon_d)-(E-\varepsilon_d)S\ . \tag{4}$$

In the vicinity of $E=\varepsilon_d$, which is the energy region of interest, the effect of S is then of second order. Thus we drop the second term in Eq. (4) and approximate $V'(E)$ by $V'(\varepsilon_d)$, which should be identified with $V_{\mathbf{k}am}$ and $V_{\mathbf{k}bm}$ in Eq. (1).

To simplify the analytic calculation, we choose $V_{\mathbf{k}m}$ to have the following model form:

$$V_{\mathbf{k}m}=V_0(k/k_0)^2\exp(-k/k_0)Y_{2m}(\theta_{\mathbf{k}},\psi_{\mathbf{k}})\ , \tag{5}$$

where V_0 and k_0 are parameters to be determined. This form is motivated by the behavior of the real atomic wave functions, which behave as r^2 at small r, and decay rapidly at large r. The model Hamiltonian thus contains three adjustable parameters, ε_d, V_0, and k_0. These will be determined by fitting to *ab initio* calculations of the d-electron counts, the width of the d-resonance peak and the overall shape of the projected d-density of states.

The electronic density of states (DOS) projected on $|d\rangle$ and $|\mathbf{k}\rangle$ states is obtained from a standard Green's-function analysis. We define a time-dependent one-electron Green's function as

$$G(E+is)=\frac{1}{E+is-H}\ , \tag{6}$$

where H is the full Hamiltonian in Eq. (1), and $s=0^{\dagger}$ is an infinitesimal, which we will take to zero in the end.

Since $\{|\alpha\rangle\}$, the combination of $\{|d\rangle\}$ and $\{|\mathbf{k}\rangle\}$ is assumed orthonormal, the density of states may be expressed as

$$\rho(E)=-\frac{1}{\pi}\text{Im}\sum_{\alpha}\langle\alpha|G|\alpha\rangle=\sum_{\alpha}\rho_{\alpha}(E)\ , \tag{7}$$

as a sum of state-projected DOS distributions.

To evaluate the diagonal elements of G, we first consider the d-d part $G_{d,d'}$ of G. Via standard multiple-scattering techniques,[24] one obtains

$$G_{dd'}=\left[E+is-H_{dd'}-\sum_{k,k'}H_{d\mathbf{k}}(E+is-H_{\mathbf{k}\mathbf{k}'})^{-1}H_{\mathbf{k}'d'}\right]^{-1}\ . \tag{8}$$

Here $H_{dd'}=\varepsilon_d\delta_{dd'}$ is a 10×10 diagonal matrix involving the ten d orbitals on the two impurities: $H_{d\mathbf{k}}=V^{*}_{\mathbf{k}d}$, $H_{\mathbf{k}\mathbf{k}'}=\varepsilon_{\mathbf{k}}\delta_{\mathbf{k}\mathbf{k}'}$, and $H_{\mathbf{k}'d'}=V_{\mathbf{k}'d'}$ are pieces of H. The 10×10 matrix $G_{dd'}$ can be decomposed into five independent 2×2 matrices, each for a different quantum number m. These are

$$G^{m}_{dd'}=\begin{bmatrix}z & z_m\\ z_m & z\end{bmatrix}^{-1}=\begin{bmatrix}\dfrac{z}{z^2-z_m^2} & -\dfrac{z_m}{z^2-z_m^2}\\ -\dfrac{z_m}{z^2-z_m^2} & \dfrac{z}{z^2-z_m^2}\end{bmatrix}\ , \tag{9}$$

where

$$z=E+is-\varepsilon_d-\Gamma(E+is)\ , \tag{10}$$

$$z_m=-\sum_{\mathbf{k}}\frac{|V_{\mathbf{k}m}|^2\exp(-i\mathbf{k}\cdot\mathbf{R})}{E+is-\varepsilon_{\mathbf{k}}}\ , \tag{11}$$

and the single-impurity self-energy

$$\Gamma(E+is)=\sum_{\mathbf{k}}\frac{|V_{\mathbf{k}m}|^2}{E+is-\varepsilon_k} \tag{12}$$

is independent of m. Thus the projected DOS on a particular orbital $|a,m\rangle$ (or $|b,m\rangle$) will be

$$\rho_m(E)=-\frac{1}{\pi}\text{Im}\langle a,m|G|a,m\rangle=-\frac{1}{\pi}\text{Im}\left[\frac{z}{z^2-z_m^2}\right]\ . \tag{13}$$

To obtain the change in the $|\mathbf{k}\rangle$-projected DOS due to the two transition-metal atoms, we write the Hamiltonian as

$$H=H_0+V\ , \tag{14}$$

where

$$H_0=\sum_{\mathbf{k}}\varepsilon_{\mathbf{k}}|\mathbf{k}\rangle\langle\mathbf{k}|+\sum_{m=-2}^{2}\varepsilon_d|a,m\rangle\langle a,m|+\sum_{m=-2}^{2}\varepsilon_d|b,m\rangle\langle b,m| \tag{15}$$

and

$$V=\left[\sum_{\mathbf{k},m}V_{\mathbf{k}am}|\mathbf{k}\rangle\langle a,m|+\sum_{\mathbf{k},m}V_{\mathbf{k}bm}|\mathbf{k}\rangle\langle b,m|\right]+\text{H.c.} \tag{16}$$

Via multiple-scattering theory, we obtain the effects of V exactly to all orders:

$$G=G_0+G_0VG_0+G_0VG_0VG_0+\cdots=G_0+G_0VG_0+G_0VGVG_0\ , \tag{17}$$

where

$$G_0=\frac{1}{E-H_0}=\sum_{\mathbf{k}}\frac{|\mathbf{k}\rangle\langle\mathbf{k}|}{E-\varepsilon_{\mathbf{k}}}+\sum_{m=-2}^{2}\frac{|a,m\rangle\langle a,m|}{E-\varepsilon_d}+\sum_{m=-2}^{2}\frac{|b,m\rangle\langle b,m|}{E-\varepsilon_d}\ . \tag{18}$$

From Eq. (17),

$$\langle\mathbf{k}|G|\mathbf{k}\rangle=\langle\mathbf{k}|G_0|\mathbf{k}\rangle+\langle\mathbf{k}|G_0VG_0|\mathbf{k}\rangle+\langle\mathbf{k}|G_0VGVG_0|\mathbf{k}\rangle\ . \tag{19}$$

The second term vanishes, and Eq. (19) reduces to

$$\langle\mathbf{k}|G|\mathbf{k}\rangle=\frac{1}{E-\varepsilon_{\mathbf{k}}}+\frac{1}{(E-\varepsilon_{\mathbf{k}})^2}\sum_{dd'}V_{kd}V^{*}_{kd'}\langle d|G|d'\rangle\ . \tag{20}$$

Here $\langle d|G|d'\rangle$ is an element of the 10×10 matrix $G_{dd'}$ in Eq. (8), with d and d' being super indices denoting both the choice of atoms and the choice of atomic d orbitals on each atom. The k-band density of states will then be

$$\begin{aligned}\rho_k&=-\frac{1}{\pi}\mathrm{Im}\sum_k\langle k|G|k\rangle=\rho_0-\frac{2}{\pi}\mathrm{Im}\sum_m\left[\sum_k\frac{|V_{km}|^2}{(E-\varepsilon_k)^2}\frac{z}{z^2-z_m^2}-\sum_k\frac{|V_{km}|^2e^{i\mathbf{k}\cdot\mathbf{R}}}{(E-\varepsilon_k)^2}\frac{z_m}{z^2-z_m^2}\right]\\&=\rho_0-\frac{2}{\pi}\mathrm{Im}\sum_m\left[\left(\frac{dz}{dE}-1\right)\frac{z}{z^2-z_m^2}-\frac{dz_m}{dE}\frac{z_m}{z^2-z_m^2}\right]\\&=\rho_0+\frac{2}{\pi}\mathrm{Im}\sum_m\frac{z}{z^2-z_m^2}-\frac{1}{\pi}\mathrm{Im}\sum_m\frac{d}{dE}\ln(z^2-z_m^2)\ .\end{aligned} \tag{21}$$

Here ρ_0 is the unperturbed free-electron density of states. The total density of states is thus

$$\begin{aligned}\rho&=\rho_k+2\sum_m\rho_m\ ,\\&=\rho_0-\frac{1}{\pi}\mathrm{Im}\sum_m\frac{d}{dE}\ln(Z^2-Z_m^2)\ .\end{aligned} \tag{22}$$

(The factor 2 in front of $\sum_m\rho_m$ comes from the fact that there are two transition-metal atoms in the system.)

We now determine the three parameters k_0, V_0, and ε_d by fitting to *ab initio* calculations the second and third moments of the projected d-DOS and the d-electron count. The *ab initio* calculations are performed using the scalar-relativistic augmented-spherical-wave (ASW) method.[25,26] They treat a single transition-metal impurity within a sixteen-atom supercell (bcc Bravais lattice) approximation. There are thirty Al atoms and two transition-metal atoms, with the latter at (0,0,0) and $a/2(1,1,1)$ in each bcc unit cell, where a is the cubic lattice constant. The lattice constant is about 8.2 Å, which means the separation between two neighboring transition-metal atoms is roughly 7.0 Å.

We define the moments of the projected DOS on a d orbital as

$$\mu_1=\int_{-\infty}^{+\infty}E\rho_d(E)dE\Big/\int_{-\infty}^{+\infty}\rho_d(E)dE\ , \tag{23}$$

$$\mu_n=\int_{-\infty}^{+\infty}(E-\mu_1)^n\rho_d(E)dE,\quad n>1\ . \tag{24}$$

μ_1 tells the position of the d-resonance peak relative to the Fermi level and is thus related to the d-electron number. μ_2 and μ_3 determine the width and shape of the peak. It may be surprising that the moments are finite, since one typically associates Lorentzian DOS distributions with impurities. However, the form [Eq. (5)] of $V_{\mathbf{k}m}$ guarantees that the induced DOS falls off as $\exp(-\text{const}\sqrt{E})$ at high energies, so that the moments are finite. In the real fitting procedure, we have to be very careful about what we mean by the d-electron number. In our calculation,

$$n_d=\int_{-\infty}^{\varepsilon_F}\rho_d(E)dE \tag{25}$$

is the quantity we can control with the parameters. But what we obtain from the *ab initio* calculations is N_d, the number of electrons with d character ($l=2$) within a certain sphere. So n_d includes some d charge outside the ASW sphere radius, and N_d includes some d-like states which, however, have a free-electron character. Before equating these two numbers, we add to N_d the number of d electrons outside the sphere, which is obtained approximately from Herman and Skillman's compilation,[27] and

then subtract from it the $l=2$ component of the free electrons inside the sphere. The Fermi energy ε_F is determined in the free-electron approximation by $N-n_d$, where N is the total number of electrons in an Al_3M unit cell. Thus ε_F and n_d must be determined self-consistently. The parameters k_0, V_0, and ε_d for the systems we have studied are listed in Table I, along with the Fermi levels and lattice constants. The results for the projected DOS on the d orbitals are shown in Fig. 1. Even though our DOS does not have nearly as many fine structures as the one from *ab initio* calculations, the overall width and shape are preserved.

Given the full density of states in Eq. (22), we readily obtain the total electronic energy of the system as a function of R, or, in other words, the pair interaction energy. Let $\rho(E,R)$ and $\rho(E,R=\infty)$ be the total densities of states corresponding to the two configurations. Then we define the pair potential as

$$V_2^{\text{eff}}(R)=2\int_{-\infty}^{\varepsilon_F}(E-\varepsilon_F)\Delta\rho(E)dE=2\int_{-\infty}^{\varepsilon_F}(E-\varepsilon_F)[\rho(E,R)-\rho(E,R=\infty)]dE$$

$$=-\frac{2}{\pi}\mathrm{Im}\sum_m\int_{-\infty}^{\varepsilon_F}(E-\varepsilon_F)\frac{d}{dE}[\ln(z^2-z_m^2)-\ln(z^2)]dE$$

$$=-\frac{2}{\pi}\mathrm{Im}\sum_m\int_{-\infty}^{\varepsilon_F}(E-\varepsilon_F)\frac{d}{dE}\ln(1-z_m^2/z^2)dE\ , \tag{26}$$

with one integration by parts, the pair potential is given by the following compact and explicit formula:

$$V_2^{\text{eff}}(R)=\frac{2}{\pi}\mathrm{Im}\sum_m\int_{-\infty}^{\varepsilon_F}\ln(1-z_m^2/z^2)dE\ . \tag{27}$$

Here the inclusion of the ε_F term inside the integrals accounts approximately for the difference between the Fermi levels corresponding to $\rho(E,R)$ and $\rho(E,R=\infty)$ (see Ref. 28); the factor of 2 in front accounts for spin degeneracy. This result is equivalent to Eq. (97) of Ref. 23 evaluated in the appropriate simplifying limits [i.e., using $E=\varepsilon_d$ in the matrix element $V'_{km}(E)$ and neglecting direct d-d interactions]. Notice that we retain only the one-electron energy in the pair potential. The justification for this comes from *ab initio* structural energy calculations,[13,14] which indicate the dominance of the one-electron energy in the structural energies. The structures of interest here contain no transition-metal nearest neighbors. Therefore, the transition-metal site d charges are expected to be fairly independent of structure, and electrostatic contributions to the structural energies should be small.

TABLE I. The three fitting parameters, the Fermi levels, and the $L1_2$ structure lattice constants. Energies given relative to the bottom of the conduction band.

	k_0(Å^{-1})	V_0 (eV)	ε_d (eV)	ε_F (eV)	a(Å)
Sc	0.605	48.5	12.80	10.44	4.11
Ti	0.587	39.2	12.04	11.08	3.99
V	0.599	34.0	11.91	11.54	3.90
La	0.824	75.5	15.43	8.66	4.46
Hf	0.752	55.4	13.63	10.63	4.08
Ta	0.773	49.5	13.00	11.19	3.98
Y	0.657	61.8	13.37	9.30	4.32
Zr	0.659	54.9	12.45	10.27	4.12
Nb	0.633	49.5	11.64	10.79	3.99
Mo	0.640	41.7	11.74	11.35	3.94
Tc	0.614	40.5	11.02	11.18	3.92
Ru	0.605	36.2	10.68	11.15	3.91
Rh	0.782	29.9	10.68	11.22	3.91
Pd	0.763	25.3	9.78	11.00	3.93
Ag	0.953	21.0	9.57	11.15	3.98

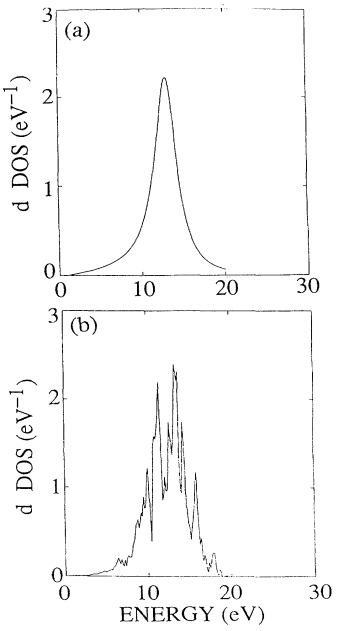

FIG. 1. (a) Model d-DOS for a single Sc impurity in Al. (b) *ab initio* d-DOS for a single Sc in Al.

RESULTS

The pair potentials for three $3d$ metals are shown in Fig. 2. Compared with the pair potentials that Moriarty obtained for V by first-principle calculations,[22] ours is much weaker. This may be connected with the fact that the Al has a higher s-p valence than the transition metals, so that the interactions may be more effectively screened. Notice also that there is no deep well in the potential corresponding to our intuitive notion of a chemical bond (Ref. 28).

As expected,[29] because of the sharp Fermi surface of Al, the calculated pair potentials have the following form at large distances:

$$V_2^{\rm eff}(R) \propto \frac{\cos(2k_F R-\delta)}{R^3}\ , \tag{28}$$

where k_F is the Fermi wave vector, and the phase shift δ is determined by the self-energy Γ at the Fermi level:

$$\delta=\tan^{-1}\left\{\frac{2[\varepsilon_d-\varepsilon_F+{\rm Re}(\Gamma)]{\rm Im}(\Gamma)}{[\varepsilon_d-\varepsilon_F+{\rm Re}(\Gamma)]^2-[{\rm Im}(\Gamma)]^2}\bigg|_{\varepsilon_F}\right\}. \tag{29}$$

[Interested readers are referred to the Appendix for the derivation of Eqs. (28) and (29).] One important feature of the pair potentials is that there are phase shifts among the curves. This plays a significant role in deciding the structural energy differences. The physical origin of the phase shifts is the difference in the number of d electrons, n_d. The term ${\rm Im}(\Gamma)$ in Eq. (29) is approximately minus the half-width of the d resonance, which does not change very much through the d series. On the other hand, the term $[\varepsilon_d-\varepsilon_F+{\rm Re}(\Gamma)]$ is positive and much larger than $-{\rm Im}(\Gamma)$ at $n_d=0$, and goes continuously to being negative and again much larger in magnitude than ${\rm Im}(\Gamma)$ at $n_d=10$. From Eq. (29), we see that δ goes continuously from 2π to 0 as n_d goes from 0 to 10. The argument of $\tan^{-1}$ and the value of δ are shown in Fig. 3.

The pair potentials can be used in a straightforward manner to calculate the structural energy differences of Al–transition-metal compounds in various structures, provided they have the same volume per atom. Here we are concerned with the relative stabilities of Al_3M in the $L1_2$ and DO_{22} structures, where M is one of the transition metals. As mentioned above, the structural energy differences are important calibration parameters for potential-energy methods for atomistic simulations. The

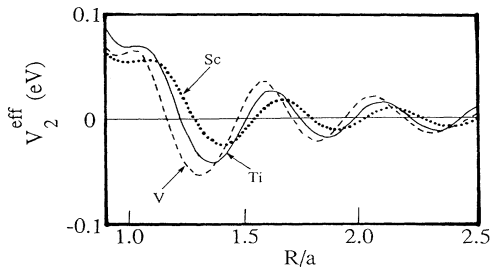

FIG. 2. Pair potentials for Sc, Ti, and V. a is the lattice constant in $L1_2$ structure.

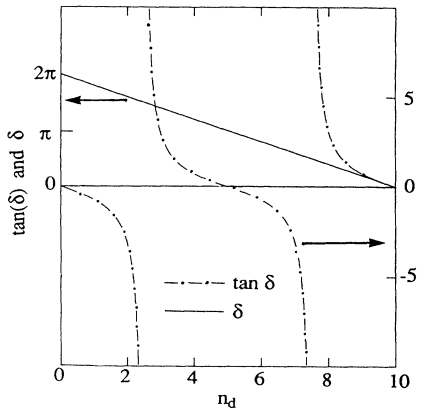

FIG. 3. Phase shift of pair potential vs d-electron number. Dash-dotted line is tanδ. Solid line is δ.

structural energies in our calculations are sums of pair potentials between transition-metal neighbors within a certain cutoff radius. The cutoff is at around 10 Å, which ensures that the first nine layers of M-M neighbors in the DO_{22} structure and the first seven in the $L1_2$ structure are included. We use a finite cutoff because a potential with a longer range than 10 Å will likely be impractical for atomistic simulations. We define the uncertainty in structural energy differences as the contributions by the layer of transition-metal atoms just beyond the cutoff radius. For Al_3V, for example, the uncertainty is about 15%. This subject will be discussed later in the paper. We first show results for the whole $4d$ row, in order to illustrate the chemical trends as completely as possible. Our results are shown in Fig. 4 along with the ASW *ab initio* results.[13] We give only numbers for the ideal c/a ratio of 2, since for most of the transition metals, the DO_{22} structure does not actually form, so one cannot measure a c/a ratio. It is clearly seen that our method works well for Nb and beyond, but not for the earlier transition metals. This is what we would expect, since the d orbitals are larger for the early transition metals, and thus the p-d covalent bonding is probably more im-

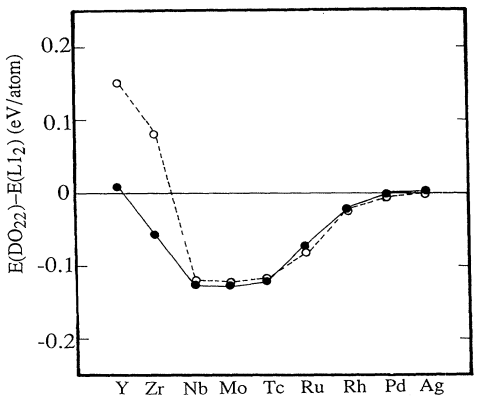

FIG. 4. Total energy differences between alternative Al_3M crystal structures, where M is a $4d$ transition metal. Open circle shows *ab initio* results. Solid circle is this work.

portant; also, three-body interactions are likely more important, because in a perturbation treatment the ratio between three-body interaction and pair interaction is proportional to V_{kd}, which is larger for the early transition metals.

Notice that the structural energy difference for Al_3Ag is zero within the accuracy of our calculation. But this does not necessarily mean that the d band is totally inert for Ag. In fact, although the potential of Ag is almost one order of magnitude smaller than that of Tc, it is by no means zero. However, it happens that the phase of the Ag potential is such that it brings Ag closer to the crossover point between the $L1_2$ and DO_{22} structures. These two effects combine to produce a very small structural energy difference.

Some of the physics behind the pair potential and the trend in structural energy differences can be understood by comparing the DOS for isolated impurities and two interacting impurities at a minimum and a maximum of the potential. Shown in Fig. 5(a) are the differences in DOS between two 4d-row impurities at a minimum of the potentials and two isolated impurities. We find a quasigap in every system and it is progressively filled up as the d band is filled up. In all the cases we show here, the DOS at the Fermi level is reduced relative to the single-impurity value. For two impurities at a maximum of the potentials, shown in Fig. 5(b), a peak is found instead around the Fermi levels. The DOS at the Fermi level is always increased relative to the single-impurity case. Thus the minima in the pair potentials seem to be caused in part by some electron transfer from just under the Fermi level to further down in the energy spectrum. For a maximum, the opposite occurs. It is satisfying that the quasigap effects, which are typically thought of in k space, can be included in an r-space description like the present one.

We have studied the extent to which orbital degeneracy is important in the model Hamiltonian. If we ignore the angular dependence of the d orbitals, we can study a pseudo-s orbital model by simply replacing Y_{2m} by Y_{00} in Eq. (5). Now we are dealing with five identical orbitals with the radial dependence of a d orbital and the angular dependence of an s orbital. The pair potentials thus obtained are more than half reduced in magnitude and the curves are out of phase with the original ones. They give the wrong chemical trend and sign of structural energy differences. For example, through most of the 4d row, the DO_{22} versus $L1_2$ structural energy difference for Al_3M is positive and has its peak value at Nb. This is in complete disagreement with the *ab initio* results in Fig. 4, and shows the importance of including orbital degeneracy. The underlying physics is that the d orbitals on the two transition-metal atoms form σ, π, and δ bonds, which give the different DOS in Fig. 5. The DOS structure then determines the pair potentials. However, the π- and δ-bonding effects are not present in the nondegenerate case, and incorrect results are obtained.

We have also calculated the structural energy differences for all the group III, IV, and V transition metals, this time including the nonideality of the c/a ratio. These have previously been treated by both the augmented-spherical-wave[13] and linear-muffin-tin-orbital[14] *ab initio* methods. Our results are shown in Fig. 6. They are consistent with the *ab initio* results in that the d-electron count is the dominant factor in deciding the structure energy differences. (Atomic size effects, for example, are not important.) They show the same overall trend as in the *ab initio* calculations, namely that the DO_{22} structure is stabilized as the d band is filled up. However, the change in the structural energy as one goes from group III to group V is about half of that in the *ab initio* calculations. In addition, the energy lowering from going to a nonideal c/a ratio is not obtained accurately. Nevertheless, the structural energies for the group V transition metals are still quite reasonable. As discussed earlier, the discrepancies between our results and the relatively accurate ones in the *ab initio* calculation are likely due to the neglect of Al pseudopotential and three-body

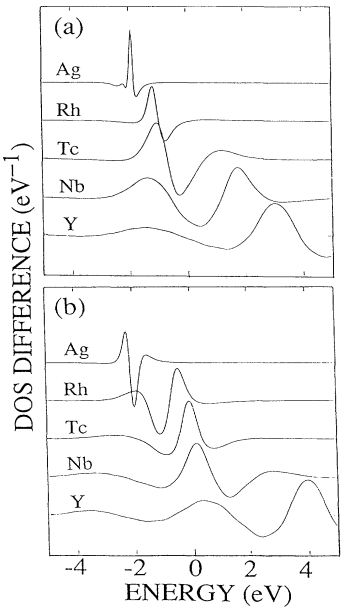

FIG. 5. DOS differences at potential minima (a) and maxima (b). Energies measured relative to Fermi levels.

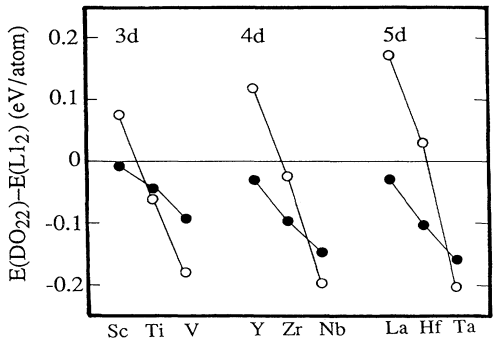

FIG. 6. Total-energy differences between alternative Al_3M structures. Open circles are *ab initio* results. Solid circles are this work. c/a ratios in DO_{22} structure are all taken to be 2.23.

interactions among the transition-metal atoms.

As mentioned above, the relevance of structural energies to extended-defect simulations lies in their connection to the antiphase boundary (APB) energies. Thus these should also be useful in the calibration of the potentials. The Al-Ti system has received the most attention here, but unfortunately our method is incapable of handling the early transition metals. For the group V metals, we know of no experimental measurements or theoretical calculations of the APB energies. However, we will present the APB results in any case, because such calculations can at least help to establish the reliability of the connection between the structural energies and the APB energies. Fairly simple examples are the (100) APB energies for Al_3V, Al_3Nb, and Al_3Ta. Here the APB is defined as a single piece of $L1_2$ packing in a system that is otherwise DO_{22}. The (100) APB energies are found to be 0.27, 0.47, and 0.44 J/m^2, respectively. In comparison, if we assume that the $L1_2$ structure is simply an array of noninteracting APB's, then we can extract numerical estimates of the APB energies from the $L1_2$-DO_{22} structural energy differences. These are 0.30, 0.48, and 0.52 J/m^2, respectively. We see a strong correlation between APB energy and structural energy difference. The discrepancy between the two sets of numbers comes from the neglect of interactions among the APB's; the small values of the discrepancies indicate that the interactions are fairly small.

MOMENT ANALYSIS

The interactions obtained above are quite long ranged, which will render simulations computationally intensive. In addition, the constant-volume constraint greatly limits the range of applicability of the potentials. For this reason, it would be useful to find a total-energy expression which contains approximately the same physics, but is shorter ranged and has a larger range of validity. A possible way of doing this is given by the moments approach. Here, one uses analytic results for the moments of the d-projected DOS to generate a model DOS from which a total energy can be calculated. For our model Hamiltonian in Eq. (1), the first few moments on a single d orbital with quantum number m are

$$\mu_2=\sum_{\mathbf{k}}|V_{\mathbf{k}m}|^2 , \tag{30}$$

$$\mu_3=\sum_{\mathbf{k}}|V_{\mathbf{k}m}|^2(\varepsilon_{\mathbf{k}}-\varepsilon_d) , \tag{31}$$

and

$$\mu_4=\left[\sum_{\mathbf{k}}|V_{\mathbf{k}m}|^2\right]^2+\sum_{\mathbf{k}}|V_{\mathbf{k}m}|^2(\varepsilon_k-\varepsilon_d)^2 + \left|\sum_{\mathbf{k}}|V_{\mathbf{k}m}|^2 e^{i\mathbf{k}\cdot\mathbf{R}}\right|^2 . \tag{32}$$

We see that the only R dependence of μ_4 comes from the third term in Eq. (32), which is always positive and zero at $R=\infty$. Thus $\mu_4(R)\geq\mu_4(R=\infty)$ for all R. Several groups[30–33] have studied the low-order moment expansion for the bonding energy of even d bands. Depending on the band-filling, the bonding energy is a simple function of the second and fourth moments of the d band. For a half filled d band, it is approximately

$$E_{\text{bonding}}\propto\mu_2\mu_4^{-1/4} . \tag{33}$$

If we ignore the fact that our $\mu_3\neq 0$ (μ_3 is always small), we would expect Eq. (33) to give us a pair potential which is always repulsive and decaying very rapidly with increasing R. In fact, a close look at the third term in Eq. (32) shows that the singularity at the origin in $\mathbf{k}$ space leads to a power law decay for large R, with the exponent being equal to $(|m|+7)$. As a result, the asymptotic behavior of E_{bonding} in Eq. (33) will be approximately $1/R^{|m|+7}$, which vanishes much more rapidly than the RKKY-type oscillations. This gives much better convergence when we calculate the structural energies. The low-order moment expansion technique turns out to be able to predict some of the chemical trends correctly. For example, the first zero crossing for the structural energy difference curve is found to be between Zr and Nb, which agrees with the *ab initio* results. In contrast, the true pair potentials predict that the zero crossing occurs between Y and Zr. The problem with the μ_4 approach is that the predicted structural energy differences are much too small. For example, the difference in μ_4 between the DO_{22} and $L1_2$ structures is about 1% of the absolute value of μ_4 for Al_3Mo, which leads to a structural energy difference of -0.01 eV/atom, while both *ab initio* and exact pair-potential calculations predict a value of -0.12 eV/atom. Notice that the potential energy contributed by the k band is not included in this approach, because it does not work for a band which is not upper bounded. However, in the exact calculation, the k-band energy is properly included, and it dominates the pair potentials at large separation. Since the structural energy differences have major contributions from long-range effects, the k band is actually the main deciding factor. In fact, the k-band contributions account for up to 80% of the structural energy differences in the system that we have studied. This is one reason why the d band-only poten-

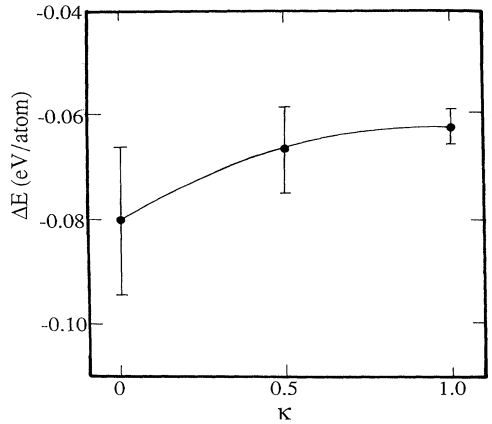

FIG. 7. Structural energy difference for Al_3V vs the decay factor κ as the calculated pair potential is multiplied by $\exp[-\kappa(R-a)/a]$.

tials in the low-order moment expansion approach predict much smaller values for the structural energy differences. Another reason is that the moments approach does not work well for a d-DOS with long tails. This is exactly the case in our situation, and it is why this approach cannot even get the d-band contribution correct. However, some recent work[34] has suggested methods of extending constant-volume potentials to situations in which the volume is not constant. If these methods can be applied to the present potentials, it may be possible to treat a much wider range of problems, such as vacancy formation and surface energies.

As mentioned above, the long range of the pair potentials can pose a serious problem for the convergence of structural energies. One simple way of circumventing this problem is to multiply the pair potentials by an exponentially decaying factor $e^{-\kappa(R-a)/a}$. This is somewhat related to doing the calculation at finite temperature. By choosing an appropriate κ, we can get rid of the long r-space tails, and at the same time retain most of the structural energies. In Fig. 7 we plot the structural energy difference of Al_3V versus κ, along with the uncertainties in ΔE caused by the sudden cutoff of the potential at about 10 Å. We can reduce the uncertainty to a quarter while ΔE is only 20% smaller.

CONCLUSION

It is satisfying that a simple pair potential of the type described here can obtain accurate estimates of the Al_3M structural energy differences for at least some of the transition metals of interest here. Future work should be directed at extending the methodology described here to the group IV transition metals, in particular the technologically important Ti. To accomplish this, it will be necessary to treat covalent p-d bonding effects more accurately. As a first step, one must include the Al pseudopotential. At least to first order, this may be computationally arduous, but not conceptually difficult; one needs only to calculate the charge density in the absence of the pseudopotential, and then evaluate the expectation value of the pseudopotential in this charge density. In addition, the greater breadth of the d bands in the early transition metals suggest that the three-body interactions should be included as well.

ACKNOWLEDGMENTS

This work was supported by the Department of Energy under Grant No. DE-FG02-84ER45130. We are grateful to Jurgen Kübler for supplying us with the relativistic ASW subroutines.

APPENDIX: DERIVATION OF THE ASYMPTOTIC BEHAVIOR OF THE PAIR POTENTIALS

From Eq. (27) we see that the asymptotic behavior of $V_2^{\rm eff}(R)$ depends on the behavior of the z_m's at large R

$$\begin{aligned} z_m(R) &= -\sum_{\mathbf{k}} \frac{|V_{\mathbf{k}m}|^2 exp(-i\mathbf{k}\cdot\mathbf{R})}{E+is-\varepsilon_{\mathbf{k}}} \\ &= \text{const}\int_0^\infty dk \frac{k^6 e^{-2k/k_0}}{E+is-\varepsilon_{\mathbf{k}}} \\ &\quad \times \int d(\cos\theta)d\psi |Y_{2m}(\theta,\psi)|^2 e^{-ikR\cos\theta} \\ &= \text{const}\int_0^\infty dk \frac{k^6 e^{-2k/k_0}}{E+is-\varepsilon_{\mathbf{k}}} g_m(kR) , \end{aligned} \tag{A1}$$

where

$$g_0(x) = 5\left[\left[\frac{1}{x}-\frac{24}{x^3}+\frac{54}{x^5}\right]\sin x+\left[\frac{6}{x^2}-\frac{54}{x^2}\right]\cos x\right] , \tag{A2}$$

$$g_{\pm1}(x) = 15\left[\left[\frac{5}{x^3}-\frac{12}{x^5}\right]\sin x+\left[-\frac{1}{x^2}+\frac{12}{x^4}\right]\cos x\right] , \tag{A3}$$

$$g_{\pm2}(x) = 15\left[\left[-\frac{1}{x^3}+\frac{3}{x^5}\right]\sin x+\left[-\frac{3}{x^4}\right]\cos x\right] . \tag{A4}$$

For large enough x, $|g_0(x)| \gg |g_{\pm1}(x)| \gg |g_{\pm2}(x)|$, so we will keep only the $m=0$ component. By using

$$\lim_{s\to0}\left[\frac{1}{x+is}\right] = P\left[\frac{1}{x}\right]-i\pi\delta(x) , \tag{A5}$$

we get

$$\begin{aligned} z_0(R) &= \text{const}\left[P\int_0^\infty dk \frac{k^6 e^{-2k/k_0} g_0(kR)}{k^2-k_E^2}+i\frac{\pi}{2}k_E^5 e^{-2k_E/k_0} g_0(k_E R)\right] \\ &\xrightarrow{R\to\infty} \text{const}\frac{1}{R}\left[P\int_0^\infty dk \frac{k^5 e^{-2k/k_0}\sin(kR)}{k^2-k_E^2}+i\frac{\pi}{2}k_E^4 e^{-2k_E/k_0}\sin(k_E R)\right] , \end{aligned} \tag{A6}$$

with $E=\hbar^2 k_E^2/2m_e$ and $\varepsilon_{\mathbf{k}}=\hbar^2 k^2/2m_e$.

There are two singularities in the integral in (A6). They determine the large-R behavior of the integral.[35] The one at $k=0$ leads to a term proportional to $1/R^6$ for large R, and the one at $k=k_E$ gives a term of order 1. So only the latter is retained and

$$z_0(R) \xrightarrow{R\to\infty} f(E)\frac{1}{R}[\cos(k_E R)+i\sin(k_E R)] = f(E)\frac{1}{R}e^{ik_E R} , \tag{A7}$$

where $f(E)$ is a smoothly varying real function of E. For very large R, Eq. (27) reduces to

$$V_2^{\text{eff}} \to -\frac{2}{\pi}\text{Im}\int_{-\infty}^{\varepsilon_F}(z_0^2/z^2)dE$$

$$\to -\frac{2}{\pi}\frac{1}{R^2}\text{Im}\int_{-\infty}^{\varepsilon_F} f(E)^2\frac{[\text{Re}(z)]^2-[\text{Im}(z)]^2-i2\,\text{Re}(z)\text{Im}(z)}{\{[\text{Re}(z)]^2+(\text{Im}(z)]^2\}^2}e^{2ik_E R}dE\ . \tag{A8}$$

The singularity at $E=\varepsilon_F$ finally gives

$$V_2^{\text{eff}}(R)\xrightarrow{R\to\infty}\text{const}\frac{\cos(2k_F R-\delta)}{R^3}\ , \tag{A9}$$

with

$$\delta=\tan^{-1}\left[\frac{2\text{Re}(z)\text{Im}(z)}{[\text{Re}(z)]^2-[\text{Im}(z)]^2}\bigg|_{\varepsilon_F}\right]=\tan^{-1}\left[\frac{2[\varepsilon_d-\varepsilon_F+\text{Re}(\Gamma)]\text{Im}(\Gamma)}{[\varepsilon_d-\varepsilon_F+\text{Re}(\Gamma)]^2-[\text{Im}(\Gamma)]^2}\bigg|_{\varepsilon_F}\right]\ . \tag{A10}$$

[1]G. Petton and D. Farkas, Scr. Metall. Mater. **25**, 55 (1991).
[2]J. Kruisman, V. Vitek, and J. Th. M. DeHosson, Acta Metall. **36**, 2729 (1988).
[3]S. P. Chen, D. J. Srolovitz, and A. F. Voter, J. Mater. Res. **4**, 62 (1989).
[4]G. J. Ackland and V. Vitek, in *High-Temperature Ordered Intermetallic Alloys III,* edited by C. T. Liu, A. I. Taub, N. S. Stoloff, and C. C. Koch (Materials Research Society, Pittsburgh, 1989).
[5]J. K. Nørskov and N. D. Lang, Phys. Rev. B **21**, 2131 (1980).
[6]M. Scott and E. Zaremba, Phys. Rev. B **22**, 1564 (1980).
[7]M. J. Puska, R. M. Nieminen, and M. Manninen, Phys. Rev. B **24**, 3037 (1982).
[8]J. K. Nørskov, Phys. Rev. B **26**, 2875 (1982).
[9]M. Manninen, Phys. Rev. B **34**, 8486 (1986).
[10]K. W. Jacobsen, J. K. Nørskov, and M. J. Puska, Phys. Rev. B **35**, 7423 (1987).
[11]M. S. Daw and M. I. Baskes, Phys. Rev. Lett. **50**, 1285 (1983).
[12]M. S. Daw and M. I. Baskes, Phys. Rev. B **29**, 6443 (1984).
[13]A. E. Carlsson and P. J. Meschter, J. Mater. Res. **4**, 1060 (1989). (For the group III-V transition metals.)
[14]J.-H. Xu and A. J. Freeman, Phys. Rev. B **40**, 11 927 (1989).
[15]A. E. Carlsson, Phys. Rev. B **40**, 912 (1989).
[16]A. Gonis, X. G. Zhang, A. J. Freeman, P. Turchi, G. M. Stocks, and D. M. Nicholson, Phys. Rev. B **36**, 4630 (1987).
[17]G. M. Stocks, in *High-Temperature Ordered Intermetallic Alloys II,* edited by N. S. Stoloff, C. C. Koch, C. T. Liu, and O. Izumi (Materials Research Society, Pittsburgh, 1987).
[18]W. A. Harrison, in *Solid State Theory* (Dover, New York, 1980).
[19]J. M. Wills and W. A. Harrison, Phys. Rev. B **28**, 4363 (1983).
[20]J. M. Wills and W. A. Harrison, Phys. Rev. B **29**, 5486 (1984).
[21]J. A. Moriarty, Phys. Rev. B **5**, 2066 (1972).
[22]J. A. Moriarty, Phys. Rev. Lett. **55**, 1502 (1985).
[23]J. A. Moriarty, Phys. Rev. B **38**, 3199 (1988).
[24]P. Roman, *Advanced Quantum Theory* (Addison-Wesley, Reading, MA, 1965), pp. 143–159.
[25]A. R. Williams, J. R. Kübler, and C. D. Gelatt, Phys. Rev. B **19**, 6094 (1979).
[26]M. Methfessel and J. R. Kübler, J. Phys. F **12**, 141 (1982).
[27]F. Herman and S. Skillman, in *Atomic Structure Calculations* (Prentice-Hall, Englewood Cliffs, NJ, 1963).
[28]A. E. Carlsson, in *Solid State Physics, Advances in Research and Applications,* Vol. 43, edited by H. Ehrenreich and D. Turnbull (Academic, New York, 1990), pp. 22, 49.
[29]See N. W. Ashcroft and N. D. Mermin, *Solid State Physics* (Holt, Rinehart, and Winston, New York, 1976), Chap. 17.
[30]R. H. Brown and A. E. Carlsson, Phys. Rev. B **32**, 6125 (1985).
[31]A. E. Carlsson and N. W. Ashcroft, Phys. Rev. B **27**, 2101 (1983).
[32]F. Ducastelle and F. Cyrot-Lackmann, J. Phys. Chem. Solids **32**, 285 (1971).
[33]F. Cyrot-Lackmann, Surf. Sci. **15**, 535 (1969).
[34]J. A. Moriarty and R. Phillips, Phys. Rev. Lett. **66**, 3036 (1991).
[35]M. J. Lighthill, *Introduction to Fourier Analysis and Generalized Functions* (Cambridge University, London, 1970).